2020 IEEE International Conference on Robotics and Automation (ICRA)
31 May - 31 August, 2020. Paris, France

Velocity Field based Active-Assistive Control for Upper Limb Rehabilitation Exoskeleton Robot

En-Yu Chia[1], Yi-Lian Chen, Tzu-Chieh Chien, Ming-Li Chiang[2], Li-Chen Fu[3], *Fellow, IEEE*, Jin-Shin Lai[4] and Lu Lu

***Abstract*— There are limitations of conventional active-assistive control for upper limb rehabilitation exoskeleton robot, such as 1). prior time-dependent trajectories are generally required, 2). task-based rehabilitation exercise involving multi-joint motion is hard to implement, and 3). assistive mechanism normally is so inflexible that the resulting exercise performed by the subjects becomes inefficient. In this paper, we propose a novel velocity field based active-assistive control system to address these issues. First, we design a Kalman filter based interactive torque observer to obtain subjects' active intention of motion. Next, a joint-position-dependent velocity field which can be automatically generated via the task motion pattern is proposed to provide the time-independent assistance to the subjects. We further propose a novel integration method that combines the active and assistive motions based on the performance and the involvement of subjects to guide them to perform the task more voluntarily and precisely. The experiment results show that both the execution time and the subjects' torque exertion are reduced while performing both given single joint tasks and task-oriented multi-joint tasks as compared with the related work in the literature. To sum up, the proposed system not only can efficiently retain subjects' active intention but also can assist them to accomplish the rehabilitation task more precisely.**

I. INTRODUCTION

Stroke is the most common neurological disorder and approximately 795,000 people suffer from a new or recurrent stroke each year [1]. The survivors of stroke may sustain from upper limb motor impairment which makes the impaired arm partially or totally paralyzed [2], [3]. These survivors require proper rehabilitation therapy to regain their motor function. Introducing the robot-assisted device into the therapy is a feasible solution to fulfill the uprising demand for treatment in the condition of increasing laborious cost. Compared with the conventional therapy provided by therapists, the robot-assisted device can offer the subject a rehabilitation exercise with reliable quality and longer duration [4].

Among different types of robot-assisted rehabilitation therapies to train various exercises, the active-assistive mode therapy, or assist-as-needed (AAN) one, is shown to be an effective way to provide the necessary assistance for stroke patients in the clinical study [5], [6]. It is also suitable for stroke patients with different levels of impairment. Thus, the research on AAN has received great attention [7]. In this mode, the robot provides the required assistance for achieving the rehabilitation task while considering the active intention of the subject. That is, if the human subjects can perform the given task well on their own, then the robot doesn't need to provide assistance. Thus, the subjects' involvement of the task can be promoted.

To implement active-assistive control, we require the control system to obtain human active intention, generate assistance based on the given task, and integrate human active intention of motion and assistance. Additional sensors such as force/torque (F/T) sensors [8], [9] or surface-electromyography (sEMG) sensors [10], [11] are utilized to obtain human intention. Nonetheless, these sensors have limitations [12]. For example, the location of F/T sensors restricts the point of human-robot interaction and a poor signal-to-noise ratio reduces reliability of sEMG sensors. To address these issues, the interactive torque observer is developed in related studies [13], [14] to estimate human intention. In [13], a Kalman filter based observer is designed to handle the uncertainties of the robot model and measurements. Besides, a nonlinear observer is employed in [14] to ensure a bounded estimation error.

In order to implement the active-assistive system, one generally needs to combine human active intention and the assistance. The generation of the assistance is closely related to the format of rehabilitation task. Normally, such task is given as a time-dependent trajectory in many related works [8]–[10], [13]–[16], which however, implies that the generated assistance compels the subjects to achieve the task-specific motion following closely the pre-specific time profiles. Some approaches have been developed to deal with this problem. In [13], a decay algorithm and an adaptive gain controller are proposed to make the subjects move slightly faster than the desired motion. The similar gain adjustment strategy is also available in [14], [16]. However, since the controller for tracking the desired timed trajectory is still dominating, the above problem is not solved well.

On the contrary, constructing a force or velocity field to represent the motion task, which is a time-independent format, has been utilized in [17]–[20]. In these studies, a joint-position-dependent force or velocity field is defined which characterizes the desired motion in terms of the position

[1]En-Yu Chia, Yi-Lian Chen and Tzu-Chieh Chien are with the Department of Electrical Engineering, National Taiwan University (NTU), Taiwan, R.O.C., r06921018@ntu.edu.tw

[2]Ming-Li Chiang is with the Graduate Institute of Automation Technology, NTUT, Taiwan, R.O.C., minglichiang@ntu.edu.tw

[3]Li-Chen Fu is with the Department of Electrical Engineering and Department of Computer Science and Information Engineering, NTU, Taiwan, R.O.C., lichen@ntu.edu.tw

[4]Jin-Shin Lai and Lu Lu are with the Department of Physical Medicine and Rehabilitation, NTU and NTU Hospital, Taiwan, R.O.C., jslai@ntu.edu.tw

978-1-7281-7395-5/20/$31.00 ©2020 IEEE

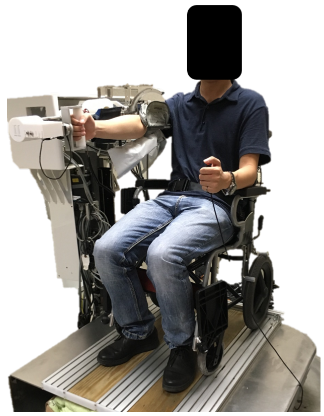

Fig. 1: NTUH-II exoskeleton robot

information. Thus, the subject's motion can be liberated from the time factor. Nevertheless, the given fields in these related studies are required to be predefined specifically, which is nontrivial especially when the multi-joint tasks. Furthermore, it needs to be altered if the desired motion is repeated or overlapped in the workspace.

To accomplish active-assistive control, human active intention and assistance from the robot are combined by torque-based integration method in many related works [10], [13]–[17], [20]. The robot controller reduces the assistance if the subject exerts the correct amount of torque to perform the task. However, it asks subjects to exert torque rather than the desired motion. A clinical report also reveals that AAN should promote the motion of performing the rehabilitation task actively rather than increase the exerted force [21].

In this paper, we propose a novel active-assistive control system which considers the mentioned issues, and implement it on the self-built exoskeleton rehabilitation robot named NTUH-II [22] as shown in Figure 1. The intention of the human subject is acquired by the designed interactive torque observer without suffering limitation of additional sensors. Besides, we design a method to automatically encode the given general rehabilitation task into a joint-position-dependent velocity field instead of time-dependent velocity field in most of the existing works in the literature. The generated assistance is time-independent, which aims to prevent dramatic limitation on the active intention of the subject. After that, we propose a novel method to integrate human active intention and assistance based on the performance and the involvement of the subject. The integrated result considers both the active intention and the given task to make subjects perform the task actively and precisely. As a result, the performance of the proposed system is verified with the stability analysis and various experiments are conducted to validate the effectiveness of the system.

The paper is organized as follows. In section II, the method for acquiring human active intention of motion, the proposed velocity field, the method for integrating active intention and assistance, the controller design and the stability analysis are presented. The experiment result is shown in section III. Finally, the conclusion is drawn in section IV.

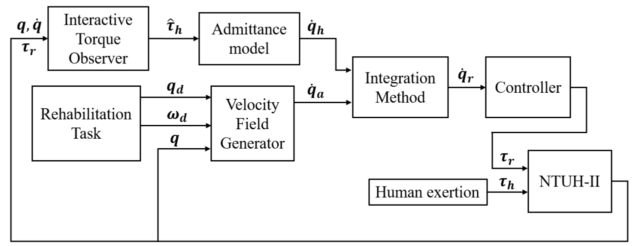

Fig. 2: The block diagram of the proposed active-assistive control system

II. Design of Active-Assistive Control System

We design the active-assistive control system to provide appropriate assistance as needed to assist the subject to accomplish the rehabilitation task. In addition, the proposed system considers the human active intention while performing the task. To evaluate our work, we apply this system to the rehabilitation robot, NTUH-II, and conduct some human testing. The system overview is shown in Figure 2. The designed Kalman filter based interactive torque observer is introduced first, which is to extract the exerted human torque reliably. Next, the admittance model is utilized to access the active motion of the human. After that, the proposed velocity field and the integration method are shown. Finally, we present the controller design and the stability analysis of the proposed system to verify the performance.

A. Kalman Filter based Interactive Torque Observer

The intention of the subject is crucial for the robot to determine the control policy. In this paper, the proposed interactive torque observer is inspired by [23] and [13] to obtain human active intention. The method in [23] is utilized to construct a linear robot dynamic model in terms of generalized momentum $\boldsymbol{p}$ to reduce the computational cost and to apply Kalman filter directly. The generalized momentum is defined as

$$\boldsymbol{p} = \boldsymbol{M}(\boldsymbol{q})\dot{\boldsymbol{q}} \tag{1}$$

and the variable $\boldsymbol{u}$ is defined as

$$\boldsymbol{u} = \boldsymbol{C}(\boldsymbol{q}, \dot{\boldsymbol{q}})^T \dot{\boldsymbol{q}} - \boldsymbol{G}(\boldsymbol{q}) - \hat{\boldsymbol{\tau}}_{\boldsymbol{f}} + \boldsymbol{\tau}_{\boldsymbol{r}}. \tag{2}$$

where $\boldsymbol{M}(\boldsymbol{q})$ is the inertia matrix; $\boldsymbol{q}$ is the joint angle; $\boldsymbol{C}(\boldsymbol{q}, \dot{\boldsymbol{q}})$, $\boldsymbol{G}(\boldsymbol{q})$ and $\boldsymbol{\tau}_{\boldsymbol{f}}$ represent the centrifugal/Coriolis matrix, gravity vector and friction vector of the robot; $\boldsymbol{\tau}_{\boldsymbol{r}}$ is the torque exerted by the motor.

By using the passivity property of the robot, $\dot{\boldsymbol{M}}(\boldsymbol{q}) - 2\boldsymbol{C}(\boldsymbol{q}, \dot{\boldsymbol{q}})$ being a skew-symmetric matrix, and the derivative of the generalized momentum, we can obtain the following linear dynamic model

$$\dot{\boldsymbol{p}} = \boldsymbol{u} + \boldsymbol{\tau}_{\boldsymbol{h}} + \boldsymbol{\omega} \tag{3}$$

where $\boldsymbol{\omega}$ represents the Gaussian noise with zero mean and covariance of $\boldsymbol{Q}$ which is introduced by the estimation of the friction [24]; $\boldsymbol{\tau}_{\boldsymbol{h}}$ is the interactive torque between human and the robot. Besides, we define the measurement $\boldsymbol{z}$ of the generalized momentum of the robot as

$$\boldsymbol{z} = \boldsymbol{p} + \boldsymbol{v} \tag{4}$$

where $\boldsymbol{v} \sim N(\mathbf{0}, \boldsymbol{R})$ is the measurement noise with zero mean and covariance of $\boldsymbol{R}$.

Then, we can directly apply Kalman filter on both (3) and (4) which yields

$$\begin{aligned} \dot{\hat{\boldsymbol{p}}} &= (\boldsymbol{u} + \hat{\boldsymbol{\tau}}_{\boldsymbol{h}}) - \boldsymbol{K}(\hat{\boldsymbol{z}} - \boldsymbol{z}) \\ \hat{\boldsymbol{z}} &= \hat{\boldsymbol{p}} \end{aligned} \tag{5}$$

where $\boldsymbol{K} = \boldsymbol{P}(\boldsymbol{P} + \boldsymbol{R})^{-1}$ is the Kalman gain and $\boldsymbol{P}$ is the covariance of the estimated error.

After that, we utilize Lyapunov analysis to construct the adaptation law of the estimated interactive torque $\hat{\boldsymbol{\tau}}_{\boldsymbol{h}}$. Let $\boldsymbol{e} = \hat{\boldsymbol{p}} - \boldsymbol{p}$ and $\boldsymbol{e}_{\boldsymbol{d}} = \hat{\boldsymbol{\tau}}_{\boldsymbol{h}} - \boldsymbol{\tau}_{\boldsymbol{h}}$. Furthermore, since there are random variables in the model, we perform the analysis on the moving average of these errors and denote them as $\bar{\boldsymbol{e}}$ and $\bar{\boldsymbol{e}}_{\boldsymbol{d}}$, respectively. Hereafter, by combing (3), (4) and (5), we can obtain the following error dynamics.

$$\dot{\bar{\boldsymbol{e}}} = -\boldsymbol{K}\bar{\boldsymbol{e}} + \bar{\boldsymbol{e}}_{\boldsymbol{d}} \tag{6}$$

Consider the following Lyapunov candidate function.

$$V_o = \frac{1}{2}\bar{\boldsymbol{e}}^T\bar{\boldsymbol{e}} + \frac{1}{2}\bar{\boldsymbol{e}}_{\boldsymbol{d}}{}^{\boldsymbol{T}}\boldsymbol{\Lambda}^{-\mathbf{1}}\bar{\boldsymbol{e}}_{\boldsymbol{d}} \tag{7}$$

where $\boldsymbol{\Lambda}$ is a diagonal positive definite matrix. We assume that the torque exerted by the subject is smooth and does not change rapidly, which is quite reasonable in rehabilitation task. Thus, the derivative of the true interactive torque approximates to zero. With this assumption, taking the derivative of (7) and performing the substitution with (6) yields

$$\dot{V}_o = -\bar{\boldsymbol{e}}^T\boldsymbol{K}\bar{\boldsymbol{e}} + \bar{\boldsymbol{e}}_{\boldsymbol{d}}{}^T(\bar{\boldsymbol{e}} + \boldsymbol{\Lambda}^{-1}\dot{\hat{\boldsymbol{\tau}}}_{\boldsymbol{h}}) \tag{8}$$

We can design the adaptation law as

$$\dot{\hat{\boldsymbol{\tau}}}_{\boldsymbol{h}} = -\boldsymbol{\Lambda}(\hat{\boldsymbol{p}} - \boldsymbol{p}) \tag{9}$$

where $\boldsymbol{\Lambda}$ controls the rate of convergence. Substituting (9) back into (8) results in

$$\dot{V}_o = -\bar{\boldsymbol{e}}^T\boldsymbol{K}\bar{\boldsymbol{e}} \tag{10}$$

By selecting the initial value of $\boldsymbol{P}$ as positive diagonal matrix and setting both $\boldsymbol{R}$ and $\boldsymbol{Q}$ to be constant positive diagonal matrices, the resulting Kalman gain $\boldsymbol{K}$ is ensured to be a diagonal positive definite matrix. Finally, follow the procedure in [13], by applying Barbalat's Lemma, we can prove that $\bar{\boldsymbol{e}} \to 0$ as $t \to \infty$. Furthermore, the estimated torque $\hat{\boldsymbol{\tau}}_{\boldsymbol{h}}$ is stable and may converge to true value with certain inputs.

B. Admittance Model

Admittance model is utilized to obtain human active intention of motion from the estimated interactive torque. In this paper, the admittance model is defined as a virtual mass-damper system which is shown as

$$\boldsymbol{M}_{\boldsymbol{h}}\ddot{\boldsymbol{q}}_{\boldsymbol{h}} + \boldsymbol{D}_{\boldsymbol{h}}\dot{\boldsymbol{q}}_{\boldsymbol{h}} = \boldsymbol{\tau}_{\boldsymbol{h}}. \tag{11}$$

where $\boldsymbol{M}_{\boldsymbol{h}}$ is the virtual mass matrix and $\boldsymbol{D}_{\boldsymbol{h}}$ is the virtual damping matrix. In this paper, $\boldsymbol{M}_{\boldsymbol{h}}$ and $\boldsymbol{D}_{\boldsymbol{h}}$ are set in diagonal form to decouple the velocities among joints, and the values are empirical. Besides, $\boldsymbol{\tau}_{\boldsymbol{h}}$ is the input which represents the human torque.

C. Velocity Field Synthesis with Rehabilitation Task

Here, we propose a method of generating time-independent assistance with the given rehabilitation task. First. we consider the task to be described as a parametric curve. For example, if a single joint task is known to be a pattern of repeated and periodical motion between two endpoints, of which the period is T and the endpoints are q_s and q_f, we can describe the task as

$$q_d(c) = \frac{(q_f - q_s)}{2}\left[1 - \cos\left(\frac{2\pi}{T}c\right)\right] + q_s \tag{12}$$

where $q_d(c)$ is the task parametric curve and c is the curve parameter, $c \geq 0$. Note that even the motion period is given, the motion pattern is what we concern and the task will become time-independent after encoding it into the velocity field. Furthermore, if we want to cope with a general task, the motion pattern of the task can be recorded during the therapist's demonstration and the method for interpolating a curve can be utilized.

After that, we encode the curve using the velocity field to make the assistance time-independent, which is inspired by a contour following application [25]. The curve parameter represents the desired target to reach on the parametric curve. Once a position is given, we can obtain a velocity from the field which aid the subject perform the correct motion pattern. In addition, with the help of the curve parameter, our designed method can even deal with a general multi-dimension task and the repeated and overlapped motions.

First, the error function which represents the deviation between the current and the desired position on the parametric curve is defined as

$$E(\boldsymbol{q}, c) = \boldsymbol{q} - \boldsymbol{q}_{\boldsymbol{d}}(c) \tag{13}$$

where $\boldsymbol{q}$ and $\boldsymbol{q}_{\boldsymbol{d}}(c)$ are the current and the desired joint angles, respectively. Then, based on the deviation, the potential function can be constructed as

$$U(E(\boldsymbol{q}, c)) = \frac{1}{2}E(\boldsymbol{q}, c)^T\boldsymbol{\Gamma}E(\boldsymbol{q}, c) \tag{14}$$

where $\boldsymbol{\Gamma}$ is a positive diagonal matrix. To minimize the deviation, we compute the negative gradient of the potential function and the result is

$$-\frac{\partial U(E(\boldsymbol{q}, c))}{\partial \boldsymbol{q}} = -\boldsymbol{\Gamma}[\boldsymbol{q} - \boldsymbol{q}_{\boldsymbol{d}}(c)]. \tag{15}$$

The direction of the equation (15) is actually the direction of the current position pointing toward the target on the desired curve $\boldsymbol{q}_{\boldsymbol{d}}(c)$. Thus, we set it as a component of the assistive velocity which guides the subject back to the desired curve. Another velocity component is needed to help subject to traverse the curve, we define it as $\boldsymbol{\omega}_{\boldsymbol{d}}(c) = \frac{d\boldsymbol{q}_{\boldsymbol{d}}(c)}{dc}$ which is the velocity on the curve. Note that this velocity can be predefined with the task.

Therefore, the assistive velocity $\dot{\boldsymbol{q}}_{\boldsymbol{a}}$ can be defined as the blending of the two velocities which is expressed as

$$\dot{\boldsymbol{q}}_{\boldsymbol{a}} = \lambda_1(\boldsymbol{q}, c)\boldsymbol{\omega}_{\boldsymbol{d}}(c) - \lambda_2(\boldsymbol{q}, c)\frac{\partial U(E(\boldsymbol{q}, c))}{\partial \boldsymbol{q}} \tag{16}$$

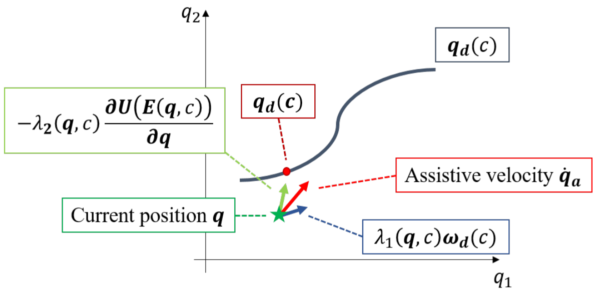

Fig. 3: Visualization of the composition of the assistive velocity

with two position-dependent coefficients $\lambda_1(\boldsymbol{q}, c)$ and $\lambda_2(\boldsymbol{q}, c)$, which are defined as

$$\lambda_1(\boldsymbol{q}, c) = \exp(-K \cdot U(E(\boldsymbol{q}, c))) \tag{17}$$

$$\lambda_2(\boldsymbol{q}, c) = 2 - \exp(-K \cdot U(E(\boldsymbol{q}, c))) \tag{18}$$

where K is a positive constant. These coefficients depend on the potential function in (14) which can be viewed as a measurement of the deviation. When the deviation is small, $\lambda_1(\boldsymbol{q}, c)$ is close to 1 which makes $\dot{\boldsymbol{q}}_{\boldsymbol{a}}$ in (16) be close to $\boldsymbol{\omega_d}$. On the contrary, if the deviation is large, $\lambda_1(\boldsymbol{q}, c)$ is close to 0 and $\lambda_2(\boldsymbol{q}, c)$ is close to 2 which makes the guidance term dominate. Figure 3 illustrates the two velocities that construct the assistive velocity $\dot{\boldsymbol{q}}_{\boldsymbol{a}}$.

Next, to construct the assistive velocity for the whole task curve, the point represented by c should be controlled to traverse through the curve. Thus, the velocity for the curve parameter is defined as

$$\dot{c} = \beta \lambda_1(\boldsymbol{q}, c) \tag{19}$$

where β is a scalar function which is defined as

$$\beta = \begin{cases} \frac{|\dot{\boldsymbol{q}}_{\boldsymbol{r}}|}{|\dot{\boldsymbol{q}}_{\boldsymbol{a}}|} & \text{if } |\dot{\boldsymbol{q}}_{\boldsymbol{a}}| \neq 0 \\ 1 & \text{otherwise.} \end{cases} \tag{20}$$

When the subject's position deviates from the desired curve, we want the subject to move toward the curve first. Hence, $\dot{c}$ is slow in this case. On the contrary, if the subject's position is close to the curve, $\dot{c}$ becomes large to make the subject traverse through the curve. Note that, since we will consider the human intention, the velocity for robot to track, which is $\dot{\boldsymbol{q}}_{\boldsymbol{r}}$, will not be the same as $\dot{\boldsymbol{q}}_{\boldsymbol{a}}$. The detail will be discussed in section II-D. Thus, the velocity for the curve parameter should also be scaled by the factor of the ratio between $\dot{\boldsymbol{q}}_{\boldsymbol{r}}$ and $\dot{\boldsymbol{q}}_{\boldsymbol{a}}$. In addition, since $\dot{\boldsymbol{q}}_{\boldsymbol{r}} = 0$ only when $\dot{\boldsymbol{q}}_{\boldsymbol{r}} = \dot{\boldsymbol{q}}_{\boldsymbol{a}} = 0$, β is always greater than 0.

D. Integration of Active Motion and Assistance

To accomplish the active-assistive control system, the velocity command to the controller should consider not only the human active motion but also the assistance. Therefore, an integration method is proposed to combine these two factors in this section. The following equation presents the proposed integration method for each joint

$$\dot{q}_{agr_i} = \alpha_i \dot{q}_{h_i} + (1 - \alpha_i)\dot{q}_{a_i}, \tag{21}$$

where $\dot{q}_{h_i}$ is the human's active motion of the i-th joint, $\dot{q}_{a_i}$ is the assistance obtained from the velocity field and $\dot{q}_{agr_i}$ is the integrated velocity.

The blending coefficient α_i for each joint relies on the involvement and the performance of the subject and is proposed to be an asymmetric bell-shaped function.

$$\alpha_i = \begin{cases} \exp\left[-\frac{1}{2}\left(\frac{\dot{q}_{h_i} - \dot{q}_{a_i}}{\sigma_{ahead}}\right)^2\right] & \text{if } (\dot{q}_{h_i}\dot{q}_{a_i}) > 0 \\ & \text{and } |\dot{q}_{h_i}| \geq |\dot{q}_{a_i}|, \\ \exp\left[-\frac{1}{2}\left(\frac{\dot{q}_{h_i} - \dot{q}_{a_i}}{\sigma_{behind}}\right)^2\right] & \text{otherwise,} \end{cases} \tag{22}$$

where σ_{ahead} and σ_{behind} can be viewed as the standard deviation of the Gaussian function. From the equation, one can observe that $\alpha_i \in [0, 1]$. If the subject are involved in the task actively and performs adequately, which means the active velocity of the subject is not too bigger or smaller than assistive velocity, a higher value of α_i will make the subject intention dominate. The asymmetric property of α_i not only encourages subjects to perform the task faster if they can but also inhibits them from performing task much slower than assistive velocity. Furthermore, we design σ_{ahead} and σ_{behind} based on the assistive motion as follows

$$\sigma_{ahead} = \delta_{ahead}\,|\dot{q}_{a_i}|\,, \sigma_{behind} = \delta_{behind}\,|\dot{q}_{a_i}| \tag{23}$$

In (23), δ_{ahead} and δ_{behind} are positive constants, where $0 < \delta_{behind} < 1$ to avoid the subject can alter the direction of the motion when the assistive velocity is slow. It is noted that σ needs to be handled specifically to avoid singularity. Equation (23) lets subjects have more freedom when assistive velocity suggests to move fast and makes subjects perform fine movement when assistive velocity is slow. Thus, the proposed method promotes subjects to accomplish the task actively while providing the necessary assistance to maintain the performance of the task execution.

To maintain the synchronization among joints when performing multi-dimension tasks, we follow the idea in [26]. Only the correct motion synergies are allowed to contribute to the motion. Thus, the vector of integrated velocities are projected onto the direction of the assistive velocity vector. The equation of the projection is given as

$$\dot{\boldsymbol{q}}_{\boldsymbol{r}} = \frac{\dot{\boldsymbol{q}}_{\boldsymbol{agr}}{}^T \dot{\boldsymbol{q}}_{\boldsymbol{a}}}{|\dot{\boldsymbol{q}}_{\boldsymbol{a}}|} \frac{\dot{\boldsymbol{q}}_{\boldsymbol{a}}}{|\dot{\boldsymbol{q}}_{\boldsymbol{a}}|}. \tag{24}$$

E. Controller Design and Stability Analysis

The controller is designed for robot to track the given velocity command to accomplish active-assistive control. First, consider the robot dynamics is given as

$$\boldsymbol{M}(\boldsymbol{q})\ddot{\boldsymbol{q}} + \boldsymbol{C}(\boldsymbol{q}, \dot{\boldsymbol{q}})\dot{\boldsymbol{q}} + \boldsymbol{G}(\boldsymbol{q}) + \boldsymbol{\tau_f} + \boldsymbol{\tau_{dis}} = \boldsymbol{\tau_r} + \boldsymbol{\tau_h} \tag{25}$$

where $\boldsymbol{\tau_{dis}}$ is the unmodeled disturbance.

Then, with the results proposed in previous subsections, the controller is designed by the standard computed torque method which is

$$\begin{aligned} \boldsymbol{\tau}_r = &\boldsymbol{M}(\boldsymbol{q})[\ddot{\boldsymbol{q}}_{\boldsymbol{r}} - \boldsymbol{K_v}(\dot{\boldsymbol{q}} - \dot{\boldsymbol{q}}_{\boldsymbol{r}}) - \boldsymbol{K_p}(\boldsymbol{q} - \boldsymbol{q_d}(c)) \\ &- \rho sgn(\dot{\boldsymbol{q}} - \dot{\boldsymbol{q}}_{\boldsymbol{r}})] + \boldsymbol{C}(\boldsymbol{q}, \dot{\boldsymbol{q}})\dot{\boldsymbol{q}} + \boldsymbol{G}(\boldsymbol{q}) + \boldsymbol{\tau_f} - \boldsymbol{\tau_h} \end{aligned} \tag{26}$$

where $\boldsymbol{K_v}$ and $\boldsymbol{K_p}$ are positive diagonal matrices. In addition, ρ is a positive constant with a lower bound $\left|\boldsymbol{M}^{-1}(\boldsymbol{q})\boldsymbol{\tau_{dis}}\right|$.

Before the stability analysis, it is worth mentioning that the ratio between $\dot{\boldsymbol{q}}_{\boldsymbol{r}}$ and $\dot{\boldsymbol{q}}_{\boldsymbol{a}}$ is in fact a scalar, which is β defined in (20), according to the projection. Besides, by (22), it ensures that the result of $\dot{\boldsymbol{q}}_{\boldsymbol{agr}}$ is limited regardless of $\dot{\boldsymbol{q}}_{\boldsymbol{h}}$ being large or small.

The Lyapunov function candidate is chosen as the following form with $\boldsymbol{e_d} = \boldsymbol{q} - \boldsymbol{q_d}(c)$, $\boldsymbol{e_r} = \dot{\boldsymbol{q}} - \dot{\boldsymbol{q}}_{\boldsymbol{r}}$ and $V = \frac{1}{2}\boldsymbol{e_d}^T\boldsymbol{K_p}\boldsymbol{e_d} + \frac{1}{2}\boldsymbol{e_r}^T\boldsymbol{e_r}$.

By taking the time derivative of V and using the relationship between $\dot{\boldsymbol{q}}_{\boldsymbol{r}}$ and $\dot{\boldsymbol{q}}_{\boldsymbol{a}}$, we obtain

$$\dot{V} = \boldsymbol{e_d}^T\boldsymbol{K_p}[\dot{\boldsymbol{q}} - \dot{\boldsymbol{q}}_{\boldsymbol{r}} + \beta\dot{\boldsymbol{q}}_{\boldsymbol{a}} - \boldsymbol{\omega_d}(c)\dot{c}] + \boldsymbol{e_r}^T\dot{\boldsymbol{e}}_{\boldsymbol{r}}. \tag{27}$$

After substituting equation (25), (26) and the designed velocity field into (27), the following derivation is obtained.

$$\begin{aligned}
\dot{V} &= \boldsymbol{e_d}^T\boldsymbol{K_p}[\boldsymbol{e_r} + \beta\lambda_1(\boldsymbol{q},c)\boldsymbol{\omega_d}(c) - \beta\lambda_2(\boldsymbol{q},c)\boldsymbol{\Gamma}\boldsymbol{e_d} \\
&\qquad - \boldsymbol{\omega_d}(c)\beta\lambda_1(\boldsymbol{q},c)] + \boldsymbol{e_r}^T\dot{\boldsymbol{e}}_{\boldsymbol{r}} \\
&= -\beta\lambda_2(\boldsymbol{q},c)\boldsymbol{e_d}^T\boldsymbol{K_p}\boldsymbol{\Gamma}\boldsymbol{e_d} - \boldsymbol{e_r}^T\boldsymbol{K_v}\boldsymbol{e_r} - \boldsymbol{e_r}^T\boldsymbol{\xi} \\
&\qquad - \rho\boldsymbol{e_r}^T sgn(\boldsymbol{e_r}) \\
&\leq -\beta\lambda_2(\boldsymbol{q},c)\boldsymbol{e_d}^T\boldsymbol{K_p}\boldsymbol{\Gamma}\boldsymbol{e_d} - \boldsymbol{e_r}^T\boldsymbol{K_v}\boldsymbol{e_r} - |\boldsymbol{\xi}|\,|\boldsymbol{e_r}| \\
&\qquad - \rho\sum_i |e_{r_i}| \\
&< 0
\end{aligned} \tag{28}$$

where the unmodeled disturbance $\boldsymbol{\xi} = \boldsymbol{M}^{-1}(\boldsymbol{q})\boldsymbol{\tau_{dis}}$ is supposed to be upper-bounded which abides by $\rho > |\boldsymbol{\xi}|$ and $\boldsymbol{\Gamma}$ is a positive diagonal matrix. Furthermore, it is ensured that $\lambda_2(\boldsymbol{q},c) > 0$ and β is always greater than 0. Thus, both $\boldsymbol{e_d}$ and $\boldsymbol{e_r}$ converges to zero asymptotically. Therefore, we can conclude that performance and safety of the proposed method is still guaranteed.

III. Experiment

To evaluate the proposed system, two experiments are performed. The first experiment verifies the system can assist the subject as needed. The second compares the proposed system with the prevalent assistive control in the related work [13]. Three healthy subjects are recruited for these experiments. The experiments are conducted with their right-side arm. During the experiment, the subject receives the visual feedback of the position information from the monitor.

A. Experiment of Assist-as-needed Property

In the first experiment, subjects are asked to perform elbow flexion/extension (EF) exercises using the proposed system. The exercise is about moving the forearm back and forth between the endpoints (0° and 60°). Subjects will change the level of involvement in the middle way before reaching the endpoint. That is, subjects try to achieve the task near the initial position but relax the arm when the joint angle is close to the endpoint. We expect the proposed system can assist the subject as needed according to different involvement levels of the subject.

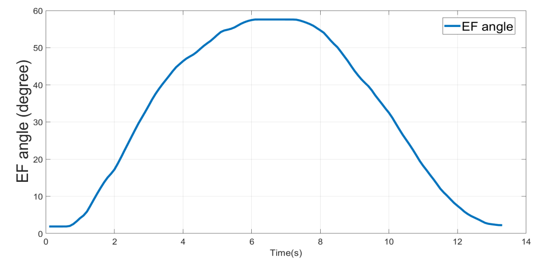

(a) Joint angle of EF task

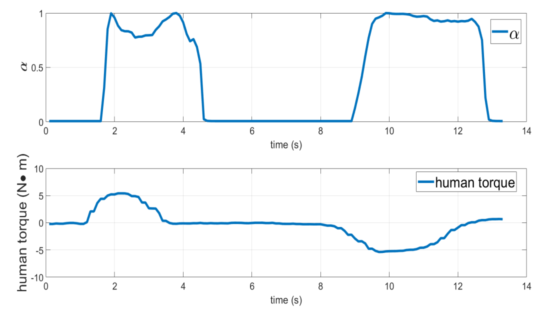

(b) Interactive torque and α of EF task

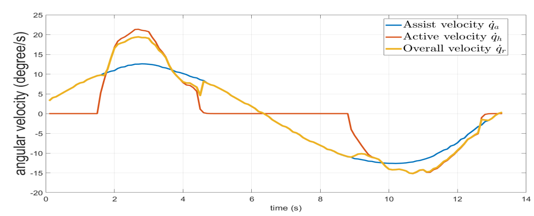

(c) Velocities of EF task

Fig. 4: The result of EF task in the first experiment

Figure 4 shows the result of performing EF task. From Figure 4b, the subject initially exerts the torque to achieve the task before about 4 seconds. Since the subject tries to perform the task with an adequate velocity, which can be seen from Figure 4c, blending coefficient α becomes nearly 1 to make subject's intention dominate. Thus, by the proposed design, the overall velocity for robot to track becomes the human active velocity. The similar phenomenon can be observed when the subject involves in the task at the time instant after 9 seconds. On the other hand, the subject relaxes the arm in between 4 to 9 seconds. Then, α drops to 0 which makes the overall velocity for robot become the assistive velocity. Thus, the given task can be accurately completed with the assistance of the robot. In conclusion, the experiment reveals that the proposed method can achieve assist-as-needed efficiently.

B. Comparison with Related Work

The second experiment is to compare the proposed system with AAN method in related work [13]. To focus on the performance of assistive control, we only implement the core part of assistive controller in [13] and the controller gain is fixed for simplicity.

Two multiple joints tasks related to activities of Daily Living (ADL) including "Raising the arm" and "Greeting"

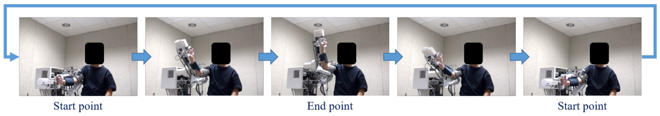

Fig. 5: The motion flow of "Raising the arm" task

TABLE I: Comparison of the average performance of multiple joints tasks with the related work for all subjects

Task	τ_{avg} (Nm)		t_{avg} (s)		ϵ_{avg} (degree)	
	Related	Ours	Related	Ours	Related	Ours
Raising the arm	5.14	2.83	11.89	10.33	1.23	0.70

are performed in this experiment. Each task will be conducted for five trials, and the subjects are asked to do their best to complete the tasks. For the limited space, we focus our following discussion on the "Raising the arm" task (Figure 5) which is composed of elbow flexion/extension (EF) and shoulder flexion/extension (SF). The full content of the experiment is shown in our video attachment.

Three metrics are utilized in this experiment. The first metric is the average of absolute interactive torque τ_{avg} which is measured from the F/T sensor on NTUH-II. The metric is used for quantifying the exertion of the subject when performing a task. The second metric is the mean absolute position error to the desired path which is defined as $\epsilon_{avg} = \frac{1}{N}\sum_n |\boldsymbol{q} - \boldsymbol{q_d}|$. N is the number of the data and $|\boldsymbol{q} - \boldsymbol{q_d}|$ represents the minimum distance to the desired path given a position. The third metric is the average execution time of a given task t_{avg}. Since our method allows the subject to move actively, we expect that the execution time using the proposed method will be shorter compared with the related work.

The experiment result is shown in Figure 6 and Table I. From Figure 6a which shows the trajectory, one can observe that the subject finishes the task earlier than the controller in [13]. It is also noted that the interactive torque using the proposed system is less than the torque in the related work, which can be seen in Figure 6b and Table I.

From the Table I, we can observe that the average performance of all subjects with the proposed system outperforms the related work. Under the same condition that subjects try their best to perform the task, the time-dependent task model and the torque-based integration method in [13] make the controller confine the subject to keep tracking the given task when the subject exert excessive torque. On the contrary, the proposed system will not restrict subjects' active intention due to the integration method proposed in Section II-D. Thus, the task can be accomplished earlier while minimizing the interactive torque. Furthermore, we also achieve satisfactory accuracy without the high-gain trade-off in the design of controller in [13] which sacrifices the human active intention.

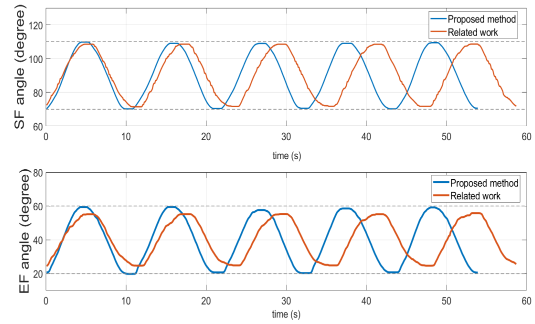

(a) Performed trajectory of the given task

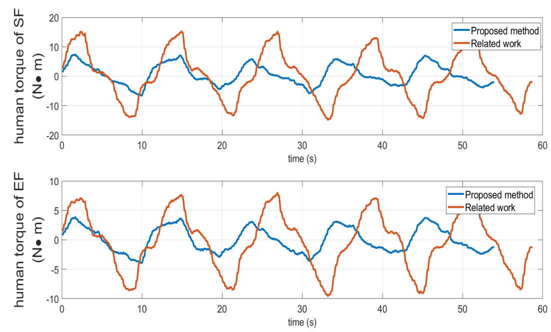

(b) Interactive torque when performing the task

Fig. 6: Results of "Raising the arm" task in the second experiment

IV. CONCLUSIONS

In this paper, a novel velocity field based active-assistive control system for upper limb rehabilitation exoskeleton robot is proposed. To realize the system, several methods are proposed. First, a Kalman filter based interactive torque observer combined with an admittance model is designed to obtain the human active intention of motion. In addition, we propose a method to generate the position based velocity field from any given task automatically to provide time-independent assistance. Finally, we propose an integration method for combining human active intention of motion and the assistance based on the subjects' involvement and performance. The method assists subjects as needed and lets them move actively when the task is performed well.

The experiment result validates that the proposed system can preserve the active intention of the subject and assist the subject as needed. Furthermore, the comparison result with the related work suggests that the subject not only can use less effort to achieve the given task but also will not be limited by the original execution time of the task. In conclusion, the proposed system can provide necessary assistance according to the subjects' intention and can assist them to accomplish given rehabilitation tasks accurately. Nonetheless, the effectiveness of the proposed method for stroke patients requires to be validated through clinical studies in the future work.

V. ACKNOWLEDGEMENT

This research was supported by the Joint Research Center for AI Technology and All Vista Healthcare under Ministry of Science and Technology of Taiwan, and Center for Artificial Intelligence & Advanced Robotics, National Taiwan University, under the grant numbers of 108-2634-F-002-017, 109-2634-F-002-027 and MOST 108-2218-E-027-014 - .

References

[1] E. J. Benjamin, P. Muntner, A. Alonso, M. S. Bittencourt, C. W. Callaway, A. P. Carson, A. M. Chamberlain, A. R. Chang, S. Cheng, S. R. Das, F. N. Delling, L. Djousse, M. S. Elkind, J. F. Ferguson, M. Fornage, L. C. Jordan, S. S. Khan, B. M. Kissela, K. L. Knutson, T. W. Kwan, D. T. Lackland, T. T. Lewis, J. H. Lichtman, C. T. Longenecker, M. S. Loop, P. L. Lutsey, S. S. Martin, K. Matsushita, A. E. Moran, M. E. Mussolino, M. OFlaherty, A. Pandey, A. M. Perak, W. D. Rosamond, G. A. Roth, U. K. Sampson, G. M. Satou, E. B. Schroeder, S. H. Shah, N. L. Spartano, A. Stokes, D. L. Tirschwell, C. W. Tsao, M. P. Turakhia, L. B. VanWagner, J. T. Wilkins, S. S. Wong, and S. S. Virani, "Heart Disease and Stroke Statistics2019 Update: A Report From the American Heart Association," *Circulation*, vol. 139, no. 10, 3 2019.

[2] J. G. Broeks, G. J. Lankhorst, K. Rumping, and A. J. Prevo, "The long-term outcome of arm function after stroke: results of a follow-up study." *Disability and rehabilitation*, vol. 21, no. 8, pp. 357–364, 8 1999.

[3] M. C. Cirstea and M. F. Levin, "Compensatory strategies for reaching in stroke." *Brain : a journal of neurology*, vol. 123, no. 5, pp. 940–953, 5 2000.

[4] V. S. Huang and J. W. Krakauer, "Robotic neurorehabilitation: a computational motor learning perspective," *Journal of NeuroEngineering and Rehabilitation*, vol. 6, no. 1, p. 5, 2009.

[5] L. E. Kahn, M. L. Zygman, W. Z. Rymer, and D. J. Reinkensmeyer, "Robot-assisted reaching exercise promotes arm movement recovery in chronic hemiparetic stroke: a randomized controlled pilot study," *Journal of neuroengineering and rehabilitation*, vol. 3, p. 12, 6 2006. [Online]. Available: https://www.ncbi.nlm.nih.gov/pubmed/16790067 https://www.ncbi.nlm.nih.gov/pmc/articles/PMC1550245/

[6] M.-H. Milot, S. J. Spencer, V. Chan, J. P. Allington, J. Klein, C. Chou, J. E. Bobrow, S. C. Cramer, and D. J. Reinkensmeyer, "A crossover pilot study evaluating the functional outcomes of two different types of robotic movement training in chronic stroke survivors using the arm exoskeleton BONES," *Journal of neuroengineering and rehabilitation*, vol. 10, p. 112, 12 2013.

[7] A. Basteris, S. M. Nijenhuis, A. H. A. Stienen, J. H. Buurke, G. B. Prange, and F. Amirabdollahian, "Training modalities in robot-mediated upper limb rehabilitation in stroke: a framework for classification based on a systematic review," *Journal of NeuroEngineering and Rehabilitation*, vol. 11, no. 1, p. 111, 2014.

[8] J. Zhang and C. C. Cheah, "Passivity and Stability of HumanRobot Interaction Control for Upper-Limb Rehabilitation Robots," *IEEE Transactions on Robotics*, vol. 31, no. 2, pp. 233–245, 2015.

[9] S. H. Chen, W. M. Lien, W. W. Wang, G. D. Lee, L. C. Hsu, K. W. Lee, S. Y. Lin, C. H. Lin, L. C. Fu, J. S. Lai, J. J. Luh, and W. S. Chen, "Assistive Control System for Upper Limb Rehabilitation Robot," *IEEE Transactions on Neural Systems and Rehabilitation Engineering*, vol. 24, no. 11, pp. 1199–1209, 2016.

[10] T. Teramae, T. Noda, and J. Morimoto, "EMG-Based Model Predictive Control for Physical HumanRobot Interaction: Application for Assist-As-Needed Control," *IEEE Robotics and Automation Letters*, vol. 3, no. 1, pp. 210–217, 2018.

[11] J. Lee, M. Kim, and K. Kim, "A control scheme to minimize muscle energy for power assistant robotic systems under unknown external perturbation," *IEEE Transactions on Neural Systems and Rehabilitation Engineering*, vol. 25, no. 12, pp. 2313–2327, 2017.

[12] L. Liu, L. Chien, S. Pan, J. Ren, C. Chiao, W. Chen, L. Fu, and J. Lai, "Interactive torque controller with electromyography intention prediction implemented on exoskeleton robot NTUH-II," in *2017 IEEE International Conference on Robotics and Biomimetics (ROBIO)*, 2017, pp. 1485–1490.

[13] A. U. Pehlivan, D. P. Losey, and M. K. O'Malley, "Minimal Assist-as-Needed Controller for Upper Limb Robotic Rehabilitation," *IEEE Transactions on Robotics*, vol. 32, no. 1, pp. 113–124, 2016.

[14] A. U. Pehlivan, D. P. Losey, C. G. Rose, and M. K. O'Malley, "Maintaining subject engagement during robotic rehabilitation with a minimal assist-as-needed (mAAN) controller," in *2017 International Conference on Rehabilitation Robotics (ICORR)*, 2017, pp. 62–67.

[15] E. T. Wolbrecht, V. Chan, D. J. Reinkensmeyer, and J. E. Bobrow, "Optimizing Compliant, Model-Based Robotic Assistance to Promote Neurorehabilitation," *IEEE Transactions on Neural Systems and Rehabilitation Engineering*, vol. 16, no. 3, pp. 286–297, 2008.

[16] T. Proietti, G. Morel, A. Roby-Brami, and N. Jarrassé, "Comparison of different error signals driving the adaptation in assist-as-needed controllers for neurorehabilitation with an upper-limb robotic exoskeleton," in *2017 IEEE International Conference on Robotics and Automation (ICRA)*, 2017, pp. 6645–6650.

[17] H. J. Asl, T. Narikiyo, and M. Kawanishi, "An Assist-as-Needed Velocity Field Control Scheme for Rehabilitation Robots," *IEEE International Conference on Intelligent Robots and Systems*, pp. 3322–3327, 2018.

[18] U. Keller, G. Rauter, and R. Riener, "Assist-as-needed path control for the PASCAL rehabilitation robot," *IEEE International Conference on Rehabilitation Robotics*, 2013.

[19] P. Agarwal and A. D. Deshpande, "Subject-Specific Assist-as-Needed Controllers for a Hand Exoskeleton for Rehabilitation," *IEEE Robotics and Automation Letters*, vol. 3, no. 1, pp. 508–515, 2018.

[20] H. J. Asl and T. Narikiyo, "An assistive control strategy for rehabilitation robots using velocity field and force field," in *2019 IEEE 16th International Conference on Rehabilitation Robotics (ICORR)*, June 2019, pp. 790–795.

[21] N. Hogan, H. I. Krebs, B. Rohrer, J. J. Palazzolo, L. Dipietro, S. E. Fasoli, J. Stein, R. Hughes, W. R. Frontera, D. Lynch, and B. T. Volpe, "Motions or muscles? Some behavioral factors underlying robotic assistance of motor recovery." *Journal of rehabilitation research and development*, vol. 43, no. 5, pp. 605–618, 2006.

[22] C. H. Lin, W. M. Lien, W. W. Wang, S. H. Chen, C. H. Lo, S. Y. Lin, L. C. Fu, and J. S. Lai, "NTUH-II robot arm with dynamic torque gain adjustment method for frozen shoulder rehabilitation," in *2014 IEEE/RSJ International Conference on Intelligent Robots and Systems*, 2014, pp. 3555–3560.

[23] A. Wahrburg, E. Morara, G. Cesari, B. Matthias, and H. Ding, "Cartesian contact force estimation for robotic manipulators using Kalman filters and the generalized momentum," in *2015 IEEE International Conference on Automation Science and Engineering (CASE)*, 2015, pp. 1230–1235.

[24] A. Wahrburg, J. Bös, K. D. Listmann, F. Dai, B. Matthias, and H. Ding, "Motor-Current-Based Estimation of Cartesian Contact Forces and Torques for Robotic Manipulators and Its Application to Force Control," *IEEE Transactions on Automation Science and Engineering*, vol. 15, no. 2, pp. 879–886, 2018.

[25] P. Y. Li and R. Horowitz, "Passive velocity field control (PVFC). Part II. Application to contour following," *IEEE Transactions on Automatic Control*, vol. 46, no. 9, pp. 1360–1371, 2001.

[26] E. B. Brokaw, R. J. Holley, and P. S. Lum, "Comparison of Joint Space and End Point Space Robotic Training Modalities for Rehabilitation of Interjoint Coordination in Individuals With Moderate to Severe Impairment From Chronic Stroke," *IEEE Transactions on Neural Systems and Rehabilitation Engineering*, vol. 21, no. 5, pp. 787–795, 2013.